Chemical Engineering Journal 163 (2010) 48–54

Contents lists available at ScienceDirect

Chemical Engineering Journal

journal homepage: www.elsevier.com/locate/cej

Effect of silicon dose on preparation and coagulation performance of poly-ferric-aluminum-silicate-sulfate from oil shale ash

Tong Sun[a,b,*], Lian-li Liu[c], Li-li Wan[c], Yan-Ping Zhang[c]

[a] Key Laboratory of Applied Chemistry, Bohai University, Jinzhou, PR China
[b] Faculty of Chemistry and Chemical Engineering, Bohai University, Jinzhou 121013, PR China
[c] Center for Science & Technology Experiment, Bohai University, Jinzhou 121013, PR China

ARTICLE INFO

Article history:
Received 22 January 2010
Received in revised form 18 July 2010
Accepted 19 July 2010

Keywords:
Coagulation
Poly-ferric-aluminum-silicate-sulfate
Oil shale ash
Sewage
Turbidity
COD

ABSTRACT

The oil shale ash was explored as a raw material for a type of new inorganic coagulant poly-ferric-aluminum-silicate-sulfate (PFASS) with various (Al + Fe)/Si molar ratios. The coagulation performances were evaluated by jar test in treating sewage, the zeta potential of the sewage was also used to evaluate the charge neutralization ability, and the microscopic images of flocs were measured by transmitting and reflecting polarizing microscope (TRPM). Meanwhile, the structure and morphology of PFASS were characterized by Infra-red spectra (FT-IR), X-ray diffraction (XRD) and transmission electron microscopy (TEM). The results of FT-IR indicate that at lower of silicon, the peaks corresponding to Fe–OH–Fe, Al–OH–Al, Fe–OH and Al–OH vibration are observable, with silicon dose further increasing, the above bonds are probably transformed to Fe–O–Fe, Al–O–Al, Fe–O and Al–O respectively, furthermore, Si–O–Fe and Si–O–Al bonds can be formed. XRD spectra illustrates that PFASS consists of $FeSO_4{\cdot}H_2O$, $NaAl(SO_4)_2{\cdot}(H_2O)_6$ and new chemical species rather than a simple mixture of the raw materials. TEM result displays that a handful of silicon is propitious to form three dimensions structure, and the chain-net is compact, however the superabundant silicon destroys the chain-net structure. The coagulant performance results illustrate that the coagulant dosage and (Al + Fe)/Si molar ratios affect the removal of turbidity and COD in sewage, as well as the turbidity removal is much larger than COD removal at the same dose.

1. Introduction

Many researches proved that the coagulant is widely used in the water and wastewater treatment facilities, especially for the destabilization of colloids suspensions and for the removal of suspended solids or organic matters [1–4]. Nearly all the colloids in wastewater carrying negative charges remain in suspension due to mutual electric repulsions. High charges cation such as, Fe^{3+} or Al^{3+} is one of the most effective ones for destabilizing the colloids. Therefore, as common inorganic coagulant, hydrolyzing metal salts based on aluminum or iron are widely used as coagulants in water and wastewater treatment. Therefore, there are a number of conventional coagulants based on aluminum or iron, such as ferric sulfate, ferric chloride, aluminum sulfate or aluminum chloride [5]. In the processes of conventional coagulation, the water temperature affects the coagulation efficiency, the formation of metal hydrolysis species is uncontrolled, the efficient coagulant dosage is large and the performance is dissatisfied. In order to solve these problems, inorganic polymer coagulant (IPC) has been developed for decades, such as poly-ferric sulfate (PFS), poly-ferric chloride (PFC) and poly-aluminum chloride (PAC) [6–9]. They contain hydrolytic and polymeric species, which make hydroxide precipitate slowly upon dilution and allow the polymeric species to be maintained for a longer duration. Moreover, IPC generally carries high positive charge to be neutralized by negative charge of the colloidal particles in water and wastewater [10]. Therefore, the performances of IPC are better than that of the conventional coagulants due to their charge neutralization capacities. Both iron and aluminum-based coagulants have distinct advantages and disadvantages for water and wastewater treatment, for this reason, the efficient coagulant is desired. So researching about IPC focus on how to avoid the drawback and improve coagulation performance of iron and aluminum-based coagulants. As we know the basic prerequisites for an effective coagulant are the charge neutralization capacity and the bridge-aggregation ability [5]. One of the methods for improving the efficiency of coagulation reagents is the addition of other components to produce new composite coagulants, such as poly-silicic acid (PS), which carries a negative charge. The main aim of this is increasing the molecular size and enhancing the

* Corresponding author at: Faculty of Chemistry and Chemical Engineering, Bohai University, Jinzhou 121013, PR China. Tel.: +86 416 3400302; fax: +86 416 3400158.
E-mail addresses: jzsuntong@sina.com, sunline710@sohu.com (T. Sun).

1385-8947/$ – see front matter.
doi:10.1016/j.cej.2010.07.037

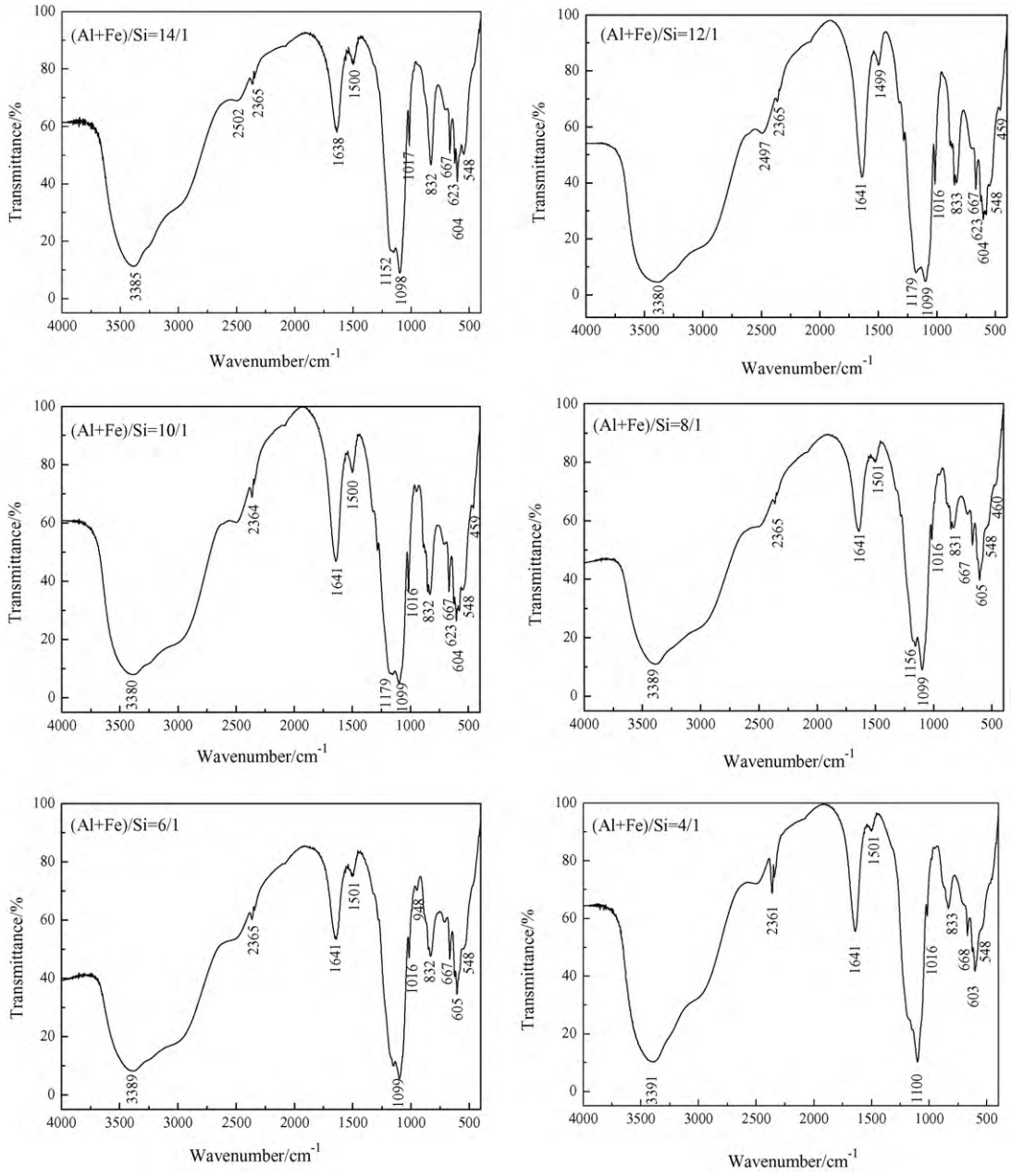

Fig. 1. FT-IR spectra of the poly-ferric-aluminum-silicate-sulfate samples with different (Al + Fe)/Si mole ratios.

bridge-aggregating ability of the coagulant, even as increasing their stability and durability [11,12]. Until now, many new IPC have been prepared and their coagulation performances have been improved, such as poly-silicate-ferric (PSiF), poly-zinc-silicate-sulfate (PZSiS), poly-ferric silicate sulfate (PFSiS), poly-ferric aluminum chloride (PFAC) [10,12–14].

Shale oil is potential alternative energy now. It is well known that China is rich in shale oil resources with 2432 million tons of mined reserves and 120 million tons of refined shale oil [15]. At the same time, a large of oil shale ash is abandoned, which consists of ferric oxide, aluminum oxide, silicon oxide and others. They were used to produce nanoscale gamma-alumina powder, zeolite, filter media, silica aerogel, silica powders, building material and so on [16–21]. But even then the high value-added products are desirous. Due to containing iron, aluminum and silicon, the oil shale ash is appropriate for producing the coagulant as raw material. However, most iron and aluminum-based coagulant manufactures use industry grade iron and aluminum ores as raw materials. Not only their capital is high, but also it would consume large quantities of the earth's limited mineral resources. Therefore, using oil shale ash to manufacture complex coagulants can result in significant savings, even more importantly, such an approach to using oil shale ash would help to conserve precious land resources and reduce the environmental degradation resulting from the storage and disposal techniques currently used in many countries.

There is limited number of studies on preparation coagulant from oil shale ash, however producing coagulant using oil shale ash as raw material will broaden the application of oil shale ash. Moreover, the poly-ferric-aluminum-silicate-sulfate (PFASS) was prepared from oil shale ash, their coagulation performance was evaluated in treating domestic sewage, the charge neutralization capacity was evaluated by zeta potential, and the microscopic images of the formed flocs were measured by TRPM. In addition, the coagulation performance of PFASS depends on some factors,

Table 1
Composition of oil shale ash.

Composition	Concentration (wt.%)
SiO_2	64.8
Al_2O_3	20.6
Fe_2O_3	8.20
MgO	1.09
K_2O	1.26
CaO	0.777
TiO_2	0.962
Na_2O	0.934
Other	1.377

such as silicon dose, alkali dose, aged time, aged temperature, etc., however it is proved that the silicon dose of PFASS is major in the pre-experiment. Therefore, in this paper, the study focuses on the influence of silicon dose on PFASS. Moreover, the structure and morphology analysis of the samples were carried out by obtaining Infra-red spectra (FT-IR), X-ray diffraction (XRD) and transmission electron microscopy (TEM) microphotographs. This study will provide a method and a useful theoretical for improving the coagulation performance of PFASS.

2. Materials and methods

2.1. Materials

All used reagents were analytically pure chemicals and deionized water with conductivity lower than 0.5 μS/cm was used to prepare all the solutions. The used oil shale ash was obtained from Fushun Mining Group Co., Ltd. (China), the manufacturer who provided the chemical properties of the oil shale ash. The composition of oil shale ash was shown in Table 1.

Sewage used in the coagulation experiments was obtained from main sewer of Bohai University (Liaoning province, China), COD of the raw water is 307 mg/L, and the turbidity is 280 NTU.

2.2. Preparation of poly-ferric-aluminum-silicate-sulfate

PFASS was prepared from the oil shale ash according to the following three steps.

2.2.1. Acid leaching

The oil shale ash with grain size lower than 120 meshes was calcinated at 650 °C for 3 h, as a result, the samples became rust red. In each acid leaching process, 100 g calcinated oil shale ash and 200 mL acid solution were added in 3 mouths flask and was stirred and heated to slight boiling (about 105 °C) for 4.5 h. The leaching liquid was separated by filtration after cooling. To wash the solid residue, the insoluble ash particles were added to 150 mL water and were stirred rapidly, and heated to 100 °C for 15 min. The resulting liquid was separated from the insoluble part by filtration after cooling. The solid residue was washed for three times in this way, and the iron and aluminum solution were mixed by mother and washing liquor and it was heated to concentrate. The solution consisted of 0.202 mol/L aluminum ion, 0.375 mol/L iron ion (0.364 mol/L Fe^{3+}, 0.011 mol/L Fe^{2+}) and less other metal ion. The concentrations of iron and aluminum were measured using VISTA-MPX ICP-OES spectroscopy (VARIAN, American), and then the concentration of Fe^{3+} and Fe^{2+} were measured by oxidation–reduction titration method.

2.2.2. Alkali leaching

First, the acid leached oil shale ash was dried at 110 °C for 2 h, then 45 g dried oil shale ash and 180 mL of 5 mol/L sodium hydroxide solution were added into the 3 mouths flask and were stirred. Second, the ash sully was heated to slight boiling (about 105 °C) for 4 h, and was separated by filtration after cooling. Finally, the residue and 150 mL water were added into 3 mouths flask and were heated to 100 °C at stirred for 15 min, and were filtered after cooling. The residue was washed in this way for three times. The mixed solution of mother and washing liquor is water glass solution with 1.65 mol/L silicate. The concentration of silicon was measured by back titration method.

2.2.3. Polymerizing

First, the water glass solution was dripped slowly into 1.6 mol/L sulfuric acid solution at 20 °C to pH 4.0 under magnetic stirring. After the solution was aged at stirring rapidly for 20 min, the solution became light blue and the PSA (poly-silicic acid) solution was obtained. Second, exact 100 mL of iron and aluminum solution was added into beaker and was heated to 50 °C, various amounts of PSA solution was added at a flow rate of 1.0 mL/min into the above solution at 50 °C under vigorous magnetic stirring to obtain different (Fe + Al)/Si mole ratios. Afterwards, 10 mL of 4 mol/L sodium hydroxide solution was dropwise added at a flow rate of 0.4 mL/min into the above solution under rapid magnetic stirring to obtain the desired r value (r = OH/(Fe + Al), about 13–14%), the solutions were aged under normal stirring at 50 °C for 3 h and PFASS coagulant was made. Finally, liquid PFASS was dried at 50 °C and was ground to make powder samples for structure analysis.

2.3. Coagulation experiments and characterization of sewage

Coagulation experiments were conducted in 1.0 L beakers using a conventional jar test apparatus (Qianjiang Meiyu Co., China). The sewages were dosed with different coagulants and stirred rapidly at 200 rpm for 1 min after adding the coagulant at 40 °C, followed by slow stir at 40 rpm for 5 min and precipitated for 20 min, in order to allow the growth of the flocs. Finally, the supernatant was withdrawn with a plastic syringe from about 2 cm below the surface of the test water for analysis. The turbidity of sewages was measured by 2100AN turbidimeter (HACH, American), and COD was measured by closed reflux method using potassium dichromate as oxidant (GB11984-89, China).

For the microscopic examination and image analysis, 1–2 drops of the coagulated water sample was placed on a microscope slide using suction tubes with a large tip to minimize breakage of flocs during transfer. The flocs were examined with BK-POLR transmitting and reflecting polarizing microscope (Chongqin Optec Instrument Co., Ltd., China). The zeta potential of pre- and post-treatment sewage was measured using ZS90 laser particle analyzer (Malvern Instruments Ltd., Britain).

2.4. Characterization of PFASS

The PFASS powder was mixed with potassium bromide and the respective pellet was prepared for FT-IR analysis. FT-IR spectroscopy was recorded with the Scimitar 2000 Near FT-IR Spectrometer (Thermo electron, USA) and the spectra were recorded in the range of 4000–400 cm^{-1}. XRD was measured for the determination of crystalline phases in solid coagulants using D/MAX-RB X-ray diffractometer (Rigaku, Japan) with Cu K-radiation in the 2θ range of 5–65° at a scan rate of 4°/min. PFASS solution was first adsorbed onto the copper net, and then dried at room temperature, and loaded to transmission electron microscope (Philips EM400T, Holland).

3. Results and discussion

3.1. FT-IR spectra analysis

Fig. 1 presents the FT-IR spectra of PFASS synthesized at respective (Al + Fe)/Si molar ratio 14/1 to 4/1. Both spectra exhibit two characteristics bonds at 3500–3300 and 1641–1638 cm^{-1}, which can be attributed to the stretching vibration of –OH and to the bending vibration of water absorbed, polymerized and crystallized in the coagulant [10,22]. Furthermore, the peaks at 2361–2365 cm^{-1} is due to carbon dioxide in air [23]. Moreover, the peaks at 1152–1179 cm^{-1} could be attributed to the asymmetric stretching vibration of Fe–O–Fe or Al–O–Al [24], 1016–1017 cm^{-1} and around 948 cm^{-1} corresponds to symmetrical stretching vibrations of Si–O–Fe and Si–O–Al respectively [25,26]. The intensity of above peaks increases with the dose of silicon increasing, and reduces when the dose is too large. In addition, there are strong absorption peaks at 1098–1100 and 831–833 cm^{-1} wave number, which are attributed to the stretching vibrations and bending vibration of Fe–OH–Fe or Al–OH–Al respectively, indicating that the polymer are formed in the samples [25,26]. The intensity of those is hardly influenced by silicon dose. In addition, the peaks at 667–668 and 623 cm^{-1} wave number are related to bending vibration of Fe–OH and Al–OH [23], it is obvious that the intensity of those decreases with the increase of silicon dose. Whereas the peaks at 603–605, 548 and 459–460 cm^{-1} may be related to the winding vibration of Si–O, Fe–O and Al–O [23,27,28], and it is shown that the peaks of Fe–O and Al–O become weak with the dose of silicon raising, furthermore, those peaks are hardly obvious at too large silicon dose.

In the case of the least of silicon dose with (Al + Fe)/Si = 14/1, the peaks corresponding to Fe–OH–Fe, Al–OH–Al, Fe–OH and Al–OH vibration are observable, with the dose of silicon increasing, the peaks become weak gradually, and they nearly disappear at low (Al + Fe)/Si mole ratio. At the same time, the peaks relating to Fe–O–Fe, Al–O–Al, Si–O–Fe, Si–O–Al, Fe–O and Al–O vibration are weak at (Al + Fe)/Si = 14/1, meanwhile, the peaks become strong with (Al + Fe)/Si mole ratio reducing, however they become weak due to excess silicon. Furthermore, the peaks of Si–O–Fe are strong but ones of Si–O–Al are hardly obvious at lower (Al + Fe)/Si mole ratio, yet, the peaks of Si–O–Fe become weak but ones of Si–O–Al become strong with the silicon dose enhancing, however, both of those are weaken when silicon dose is too large. The results indicate that Fe–OH–Fe, Al–OH–Al, Fe–OH and Al–OH bonds are probably transformed to Fe–O–Fe, Al–O–Al, Fe–O and Al–O respectively, furthermore the bonds connect with Si to form Si–O–Fe and Si–O–Al bonds. However, comparing the peaks of Si–O–Fe and Si–O–Al possibility be explained that Fe–O–Fe and Fe–O connect with Si to form the Si–O–Fe bonds when silicon is added into the solution at first. In the process of adding silicon continually, Al–O–Al and Al–O bonds connect with Si to form Si–O–Al bonds and some of Si–O–Fe bonds are instead of Si–O–Al. The redundant silicon is unfavorable for formation of Si–O–Fe and Si–O–Al. Overall, the findings of FT-IR analysis support the statement that new chemical species consisting of iron, aluminum and silica are formed, which is in total agreement with the conclusion withdrawn from XRD analysis. Furthermore, it is evident that (Al + Fe)/Si mole ratio has a significant role on the structure of PFASS coagulants. Above analysis probably suggests that PFASS is not a simple mixture of raw materials but a complex compound by iron, aluminum and silicon.

3.2. XRD analysis

Fig. 2 illustrates the XRD spectra of the powder PFASS samples with different (Al + Fe)/Si molar ratios. As shown in Fig. 2, the results show that PFASS consist of $FeSO_4{\cdot}H_2O$, $NaAl(SO_4)_2{\cdot}(H_2O)_6$ and other crystal. As Fu [22] suggests that the reaction rate of Fe^{2+} with PSA is very slow, so the reaction between Fe^{2+} and Si can be neglected here, furthermore, the mode of Fe^{2+} is $FeSO_4{\cdot}H_2O$ crystal in the samples. Additionally, a detailed study of the peaks reveals that a new compound has been formed (at $2\theta = 17.4^\circ$, 23.7°, 25.3°, 37.4° and 41.0°), and the diffractive crystals spectra such as $Fe_2(SO_4)_3$, $Al_2(SO_4)_3$, Fe_2O_3, Al_2O_3, $Fe(OH)_3$, $Al(OH)_3$, Fe_3O_4 and SiO_2 cannot be observed, which indicates that such materials as Fe^{3+}, Al^{3+}, $SO_4{}^{2-}$ and Si have been polymer to form a new compound excluded in the XRD card or a new matter not given a standard molecular formula. At the same time, the XRD spectra show that the intensity and 2θ of the peaks are slightly different with different (Al + Fe)/Si molar ratios. It is demonstrated that the crystal of PFASS had a little change due to difference of (Al + Fe)/Si molar ratios. Therefore, XRD studies indicate that the addition of PSA into the iron and aluminum mixed solution possibly leads to the formation of Fe–O–Fe, Al–O–Al, Si–O–Fe and Si–O–Al bonds to some extent, suggesting that PFASS contains new chemical species rather than a simple mixture of the raw materials. The aforementioned suggestion agrees with those of Fu and Moussas et al. [22,25], although powder PFASS were produced with different preparation methods. At the same time, the results are corresponded to FT-IR results.

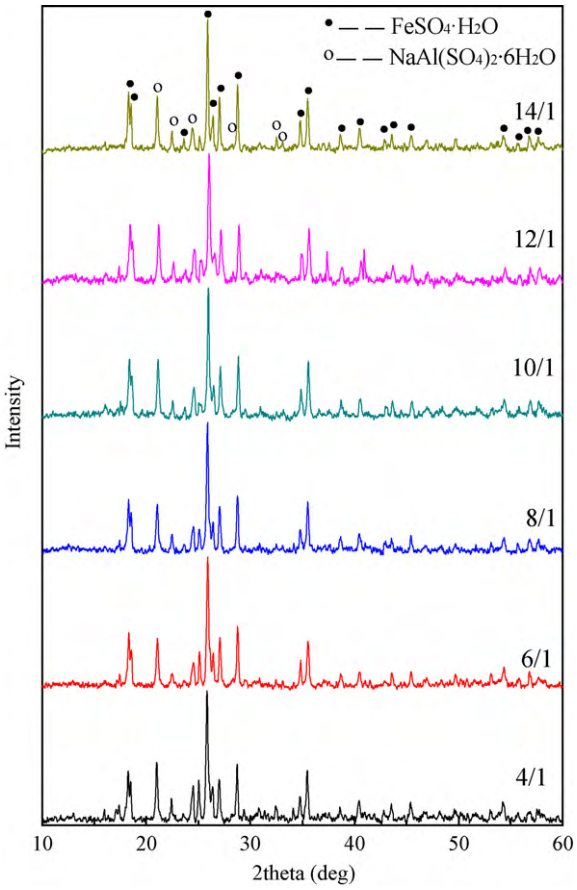

Fig. 2. XRD spectra of the poly-ferric-aluminum-silicate-sulfate samples with different (Al + Fe)/Si mole ratios.

3.3. TEM microphotographs analysis

Fig. 3 displays the TEM micro morphology of PFASS and it is shown that the microstructure of PFASS is different due to different (Al + Fe)/Si molar ratios. As discussed previously, the structure of PFASS coagulants is affected by (Al + Fe)/Si molar ratio. As shown in Fig. 3, a chain-net structure with three dimensions appears when

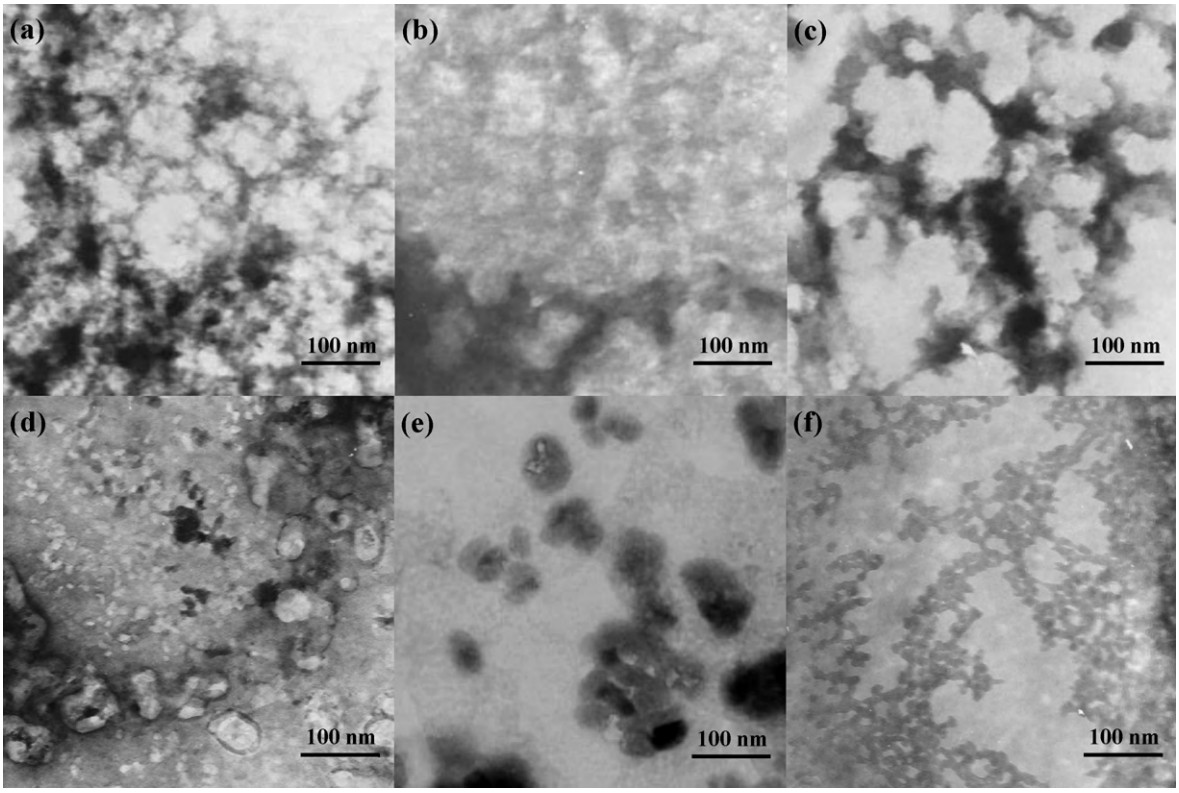

Fig. 3. TEM microphotographs of the poly-ferric-aluminum-silicate-sulfate with different (Al + Fe)/Si mole ratios. (a) (Al + Fe)/Si = 14/1; (b) (Al + Fe)/Si = 12/1; (c) (Al + Fe)/Si = 10/1; (d) (Al + Fe)/Si = 8/1; (e) (Al + Fe)/Si = 6/1; (f) (Al + Fe)/Si = 4/1.

(Al + Fe)/Si mole ratio is 14/1, that is to say, a handful of silicon is propitious to form three dimensions structure, as well as the chain-net is compact. Furthermore, with the increase of silicon dose, the structure of the PFASS makes a difference. When (Al + Fe)/Si mole ratio reduces to 12/1 or 10/1, the chain-net structure becomes coarser microstructures, the chain becomes thick and the hole of net becomes bigger than the former. And further increasing silicon dose in PFASS, the chain-net structure with three dimensions is broken gradually. The aggregate structure appears instead of a part of chain-net structure at 8/1 or 6/1 (Al + Fe)/Si mole ratio. However, the new type of chain-net appears with 4/1 (Al + Fe)/Si mole ratio, which is comprised of granular structure, it is similar to PSA [29]. The above indicates that the superabundant silicon destroys the chain-net structure. As a result, it may be unfavorable to a bridging ability of the samples.

3.4. Coagulation performance

Coagulation experiments were also conducted for the evaluation of PFASS capability with different (Al + Fe)/Si molar ratios to treat sewage by the removal of turbidity and COD, and the results are given in Fig. 4. Meanwhile, the zeta potentials of the sewage which is influenced by coagulant are shown in Fig. 5. The coagulation efficiency and mechanisms of PFASS are compared in terms of turbidity, COD removal as well as zeta potential in this study. The results illustrate that coagulant dosage affects the removal of turbidity and COD. From Fig. 4, it can be seen that the coagulation efficiency is improved with the increase of coagulant dosage in lower dose, conversely, when the coagulant dose exceeds the effective dosage, the removal of turbidity and COD reduces. The suitable coagulant dosage is in the range of 60–80 mg/L for the tur-

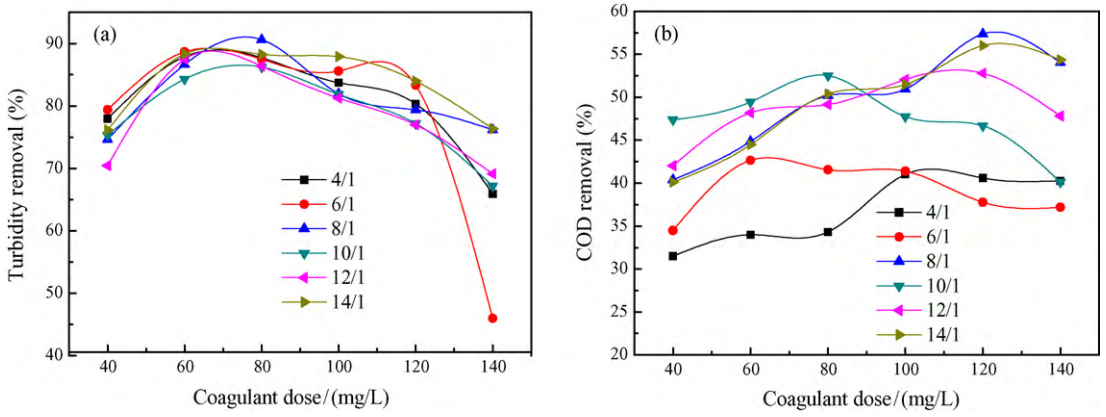

Fig. 4. Coagulation efficiency of PFASS with different (Al + Fe)/Si mole ratios on turbidity and COD.

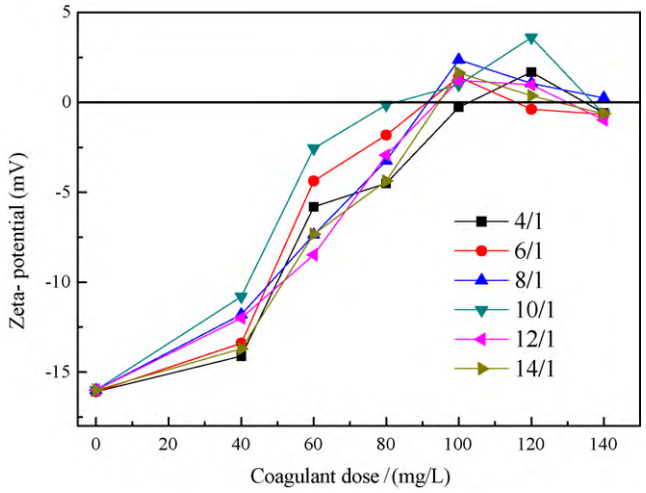

Fig. 5. Influence of coagulant dose on the zeta-potential of sewage with different (Al + Fe)/Si mole ratios.

bidity removal, and the suitable dose is uncertain for COD removal. The zeta potential increase gradually with PFASS dose increasing, and then the rate of increasing is different due to different (Al + Fe)/Si mole ratios. It is shown that the charge neutralization ability of PFASS presents a slight rise as (Al + Fe)/Si mole ratio further increases, and the optimal (Al + Fe)/Si mole ratio is 10/1. As (Al + Fe)/Si mole ratio further increases, the charge neutralization ability decreases. The similar observation was seen by Moussas and Zouboulis [25]. However, when the dose further increases, the zeta potential is apt to move into positive side, and turbidity and COD removal decrease due to the restabilization of particles.

It is known that the coagulation by hydrolyzing metal salts is generally described as a combination of charge neutralization, entrapment, adsorption and complexation with coagulant metal hydrolysis species into insoluble particulate aggregates [5,30]. Fig. 5 shows that zeta potential of sewage increases with coagulant dosage increasing, but it is also noteworthy that the optimal values of turbidity or COD removal efficiencies are not always close to the isoelectric point. As a result, it probably implies that coagulation is not completely attributed to the charge neutralization, but it is also due to synthesized function of adsorption, entrapment, and complexation. At the same time, the positive charge of hydrolyzate charges neutrality with the opposite charge of colloidal particles in sewage, due to charge neutralization of PFASS. As the dose is 40 mg/L, PFASS do not effectively remove turbidity and COD, because there are not enough hydrolyzate and positive charge supplied by PFASS to form the initial flocs, so that it leads to low coagulation efficiency. At 60–80 mg/L dose, the turbidity removals are bigger than others, however, the zeta potential have not attain to the isoelectric point, which possibly suggests that entrapment, adsorption and bridging play important roles instead of charge neutralization in coagulation process. The results are not accordant to Wei et al. [30]. However, the excessive dosage of coagulant leads to more and more PFASS being adsorbed on the initial floc surface. As every colloidal particle adsorbs redundant PFASS, there are not unoccupied surface to bridge. At the same time the excessive positive charge on the hydrolysate baffles PFASS to be adsorbed onto the initial flocs, which goes against the formation of large flocs. As a result, the turbidity and COD removal decrease.

Fig. 4 also shows that the coagulation efficiency in sewage improves with the increase of (Al + Fe)/Si mole ratio of PFASS, however, the coagulation efficiency reduces because of the exceeded (Al + Fe)/Si mole ratio, and then the influence rate to COD removal is greater than turbidity removal. The turbidity removal of PFASS with 6/1 or 8/1 (Al + Fe)/Si mole ratio is slight finer than others, meanwhile, the COD removal of PFASS with 10/1 (Al + Fe)/Si mole ratio is the optimal at lower dose (80 mg/L), and 8/1 (Al + Fe)/Si mole ratio is the optimal at higher dose (120 mg/L), as well as it is obvious that higher (Al + Fe)/Si mole ratio is favor to remove COD in sewage. In order to further study the coagulation performance of PFASS, the microscopic images of the flocs formed in the sewage at different (Al + Fe)/Si mole ratios is measured, and the results are shown in Fig. 6. According to the flocs micrographs result, it can be concluded that the flocs are formed with chain-net structure, and the size of flocs reduces with (Al + Fe)/Si mole ratio, as (Al + Fe)/Si mole ratio is 14/1, the floc is bigger than others, and then the flocs become thinner and fluffier gradually with (Al + Fe)/Si mole ratio decreasing, and this goes against sedimentation of flocs. Nevertheless, 4/1

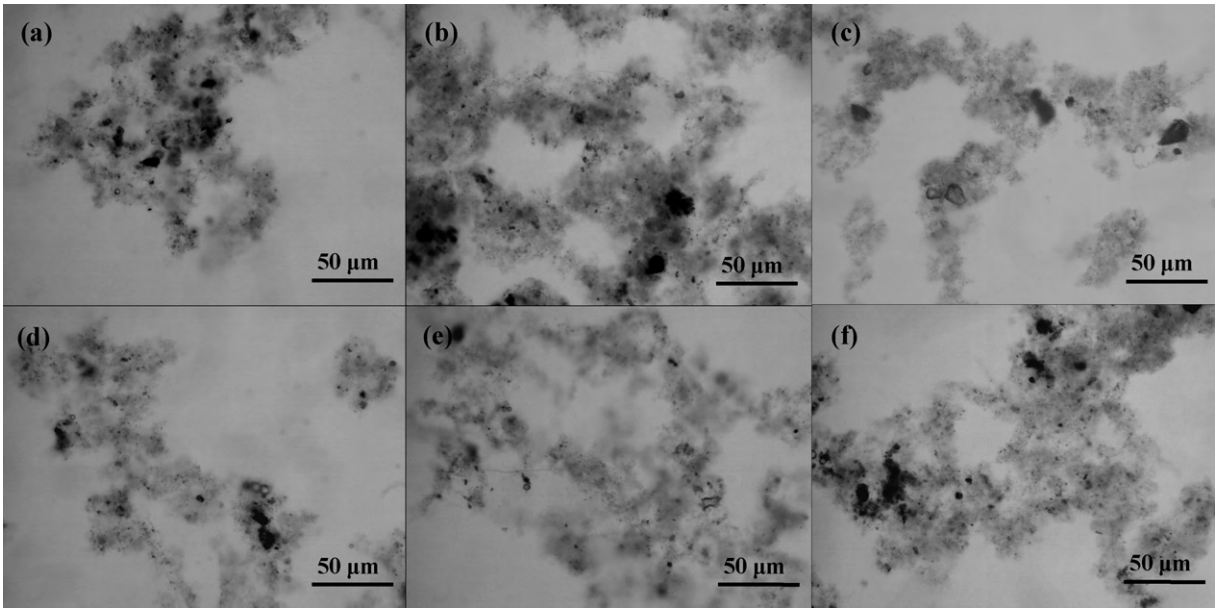

Fig. 6. Micrographs of the flocs formed in sewage at different (Al + Fe)/Si mole ratios. (a) (Al + Fe)/Si = 14/1; (b) (Al + Fe)/Si = 12/1; (c) (Al + Fe)/Si = 10/1; (d) (Al + Fe)/Si = 8/1; (e) (Al + Fe)/Si = 6/1; (f) (Al + Fe)/Si = 4/1.

(Al + Fe)/Si mole ratio makes the flocs grow dense. The observation suggests that the microscopic images of the flocs are influenced by micro-structure of PFASS (Fig. 3).

Above results probable suggest that at higher (Al + Fe)/Si mole ratio, the better chain-net structure of PFASS lead to stronger absorption bridging ability. Instead, at lower (Al + Fe)/Si mole ratio, exceeded silicon results in chain-net structure of PFASS destroyed, and then the absorption bridge ability is lower than before. At the same time, all coagulants have slightly different charge neutralizations. For this reason, COD is probably removed mainly by combination of bridge formation and sweep coagulation mechanisms. However, the similar turbidity removal for all PFASS indicates that the turbidity is removed mainly by charger neutralization ability.

Furthermore, as is shown in Fig. 4, the turbidity removal is much larger than COD removal at the same dose, and the results indicate that the maximum turbidity reduction is above 90%, and the maximum COD reduction reaches 57%, this corresponds to some previous studies [30,31]. In coagulation process, the charge of colloidal particles is neutralized with coagulant, and organic matter is adsorbed by hydrolysis species to form the original flocs before being removed, and the original flocs grow gradually. Above results probably suggest that the organic flocs formation is slower than charge neutralization.

4. Conclusions

New inorganic coagulant PFASS with various (Al + Fe)/Si molar ratios was successfully prepared from oil shale ash. It is found that PFASS contains new chemical species rather than a simple mixture of the raw materials, and the structure of the samples is effected by (Al + Fe)/Si molar ratio. At lower of silicon dose, the peaks corresponding to the Fe–OH–Fe, Al–OH–Al, Fe–OH and Al–OH vibration are observable, with silicon dose increasing, these bonds are probably transformed to Fe–O–Fe, Al–O–Al, Fe–O and Al–O respectively, the Si–O–Fe and Si–O–Al bonds can be also formed. A little silicon is propitious to the formation of three-dimensional structure, however, the superabundant silicon destroys the china-net structure. The coagulation results also demonstrated that the coagulation efficiency is affected by the coagulant dosage and (Al + Fe)/Si molar ratios. The suitable coagulant dosage is in the range of 60–80 mg/L for turbidity removal, and the suitable dose is uncertain for COD removal. The suitable (Al + Fe)/Si mole ratio is 6/1 or 8/1 for turbidity removal, and higher (Al + Fe)/Si mole ratio is favor to remove COD in sewage. As well as the turbidity removal is much larger than COD removal at the same dose. COD is probable removed mainly by the combination of bridge formation and sweep coagulation mechanisms, in the same way the turbidity is removed mainly by charger neutralization ability.

Acknowledgements

This study was financially supported by the Project of Natural Science Foundation of Liaoning Province, China (20092193) and the Project of Education Department of Liaoning Province, China (2009A043).

References

[1] A.I. Zouboulis, P.A. Moussas, F. Vasilakou, Polyferric sulphate: preparation, characterization and application in coagulation experiments, J. Hazard. Mater. 155 (2008) 459–468.
[2] P.A. Moussas, A.I. Zouboulis, A new inorganic–organic composite coagulant, consisting of polyferric sulphate (PFS) and polyacrylamide (PAA), Water Res. 43 (2009) 3511–3524.
[3] B.-Y. Gao, Y. Wang, Q.-Y. Yue, J.-C. Wei, Q. Li, Color removal from simulated dye water and actual textile wastewater using a composite coagulant prepared by ployferric chloride and polydimethyldiallylammonium chloride, Sep. Purif. Technol. 54 (2007) 157–163.
[4] G.D. Feo, S.D. Gisi, M. Galasso, Definition of a practical multi-criteria procedure for selecting the best coagulant in a chemically assisted primary sedimentation process for the treatment of urban wastewater, Desalination 23 (2008) 229–238.
[5] F.-T. Li, S.-F. Zhang, Y. Zhao, Coagulant and Flocculating Agent, Chemical Industry Press, Beijing, 2005.
[6] J.-Q. Jiang, N.J.D. Graham, Observations of the comparative hydrolysis/precipitation behaviour of polyferric sulphate and ferric sulphate, Water Res. 32 (1998) 930–935.
[7] J.-Q. Jiang, N.J.D. Graham, Preliminary evaluation of the performance of new pre-polymerised inorganic coagulants for lowland surface water treatment, Water Sci. Technol. 37 (1998) 121–128.
[8] H.-X. Tang, W. Stumm, The coagulating behaviors of Fe(III) polymeric species—II. Preformed polymers in various concentrations, Water Res. 21 (1987) 123–128.
[9] Y.-H. Shen, B.A. Dempsey, Synthesis and speciation of polyaluminum chloride for water treatment, Environ. Int. 24 (1998) 899–910.
[10] Y.-B. Zeng, J. Park, Characterization and coagulation performance of a novel inorganic polymer coagulant poly-zinc-silicate-sulfate, Colloid Surf. A 334 (2009) 147–154.
[11] D.-S. Wang, H.-X. Tang, Modified inorganic polymer flocculant-PFSi: its preparation, characterization and coagulation behavior, Water Res. 35 (2001) 3418–3428.
[12] Y. Fu, S.-L. Yu, C.-W. Han, Morphology and coagulation performance during preparation of poly-silicic-ferric (PSF) coagulant, Chem. Eng. J. 149 (2009) 1–10.
[13] X. Xu, S.-L. Yu, W.-X. Shi, Z.-Q. Jiang, C. Wu, Effect of acid medium on the coagulation efficiency of polysilicate-ferric (PSF)—a new kind of inorganic polymer coagulant, Sep. Purif. Technol. 66 (2009) 486–491.
[14] W.-P. Cheng, F.-H. Chi, C.-C. Li, R.-F. Yu, A study on the removal of organic substances from low-turbidity and low-alkalinity water with metal–polysilicate coagulants, Colloid Surf. A 312 (2008) 238–244.
[15] http://www.cppei.org.cn/xmgc_text.asp?id=8378&classid=1.
[16] B.-C. An, W.-Y. Wang, G.-J. Ji, S.-C. Gan, G.-M. Gao, J.-J. Xu, G.-H. Li, Preparation of nano-sized α-Al_2O_3 from oil shale ash, Energy 35 (2010) 45–49.
[17] S. Reyad, A.-H. Adnan, H. Malik, K. Abdelaziz, Conversion of oil shale ash into zeolite for cadmium and lead removal from wastewater, Fuel 83 (2004) 981–985.
[18] A. Kaasik, C. Vohla, R. Mõtlep, Ü. Mander, K. Kirsimäe, Hydrated calcareous oil-shale ash as potential filter media for phosphorus removal in constructed wetlands, Water Res. 42 (2008) 1315–1323.
[19] G.-M. Gao, D.-R. Liu, H.-F. Zou, L.-C. Zou, S.-C. Gan, Preparation of silica aerogel from oil shale ash by fluidized bed drying, Powder Technol. 197 (2010) 283–287.
[20] G.-M. Gao, H.-F. Zou, D.-R. Liu, L.-N. Miao, S.-C. Gan, B.-C. An, J.-J. Xu, G.-H. Li, Synthesis of ultrafine silica powders based on oil shale ash by fluidized bed drying of wet-gel slurry, Fuel 88 (2009) 1223–1227.
[21] S.Y.N. Chan, X.-H. Ji, Water sorptivity and chloride diffusivity of oil shale ash concrete, Constr. Build. Mater. 12 (1998) 177–183.
[22] Y. Fu, S.-L. Yu, Y.-Z. Yu, L.-P. Qiu, B. Hui, Reaction mode between Si and Fe and evaluation of optimal species in poly-silicic-ferric coagulant, J. Environ. Sci. 19 (2007) 678–688.
[23] Y.-M. Fang, X.-D. Zhao, X.-L. Zhang, Study on the image, structure and coagulation behavior of polysilicate-aluminum ferric, Ind. Safety Environ. Prot. 10 (2007) 22–24.
[24] B.-Y. Gao, L.-L. Liu, W.Z. Zhou, Q.Y. Yue, Q. Li, Study on the hydrolysis-polymerization process of aluminum in polyaluminum silicate chloride (PASC) flocculant, Acta Sci. Circum. 11 (2005) 1464–1469.
[25] P.A. Moussas, A.I. Zouboulis, A study on the properties and coagulation behaviour of modified inorganic polymeric coagulant—polyferric silicate sulphate (PFSiS), Sep. Purif. Technol. 63 (2008) 475–483.
[26] F.-S. Zhou, S.-H. Wang, J.-Z. Su, H. Sun, P. Zhu, J. Ding, Y.-Z. Xu, J.-G. Wu, The infrared spectra and characteristics of PMC—a multicore inorganic polymer flocculant, Fine Chem. 10 (2003) 615–618.
[27] Y.-M. Fang, Study on properties and coagu-flocculation mechanism of green flocculant PAS, Chin. J. Environ. Eng. 11 (2009) 2021–2025.
[28] S. Mohan, R. Gandhimathi, Removal of heavy metal ions from municipal solid waste leachate using coal fly ash as an adsorbent, J. Hazard. Mater. 169 (2009) 351–359.
[29] H. Liu, S. Jun, J. Liang, J. Wen, Image and flocculation mechanism of polyaluminum silicate sulfate, Chin. J. Environ. Eng. 4 (2008) 476–481.
[30] J.-C. Wei, B.-Y. Gao, Q.-Y. Yue, Y. Wang, L. Lu, Performance and mechanism of polyferric-quaternary ammonium salt composite flocculants in treating high organic matter and high alkalinity surface water, J. Hazard. Mater. 165 (2009) 789–795.
[31] W. Lan, H.-Q. Qiu, J. Zhang, Y.-J. Yu, K.-L. Yang, Z.-Z. Liu, G.-J. Ding, Characteristic of a novel composite inorganic polymer coagulant–PFAC prepared by hydrochloric pickle liquor, J. Hazard. Mater. 162 (2009) 174–179.